Phys. Status Solidi A **211,** No. 5, 1062–1066 (2014) / **DOI** 10.1002/pssa.201300762

Part of Topical Section on
Nanoscaled Magnetism and Applications

physica status solidi a
www.pss-a.com
applications and materials science

The effects of spark plasma sintering consolidation on the ferromagnetic resonance spectra (FMR) of Ni–Zn ferrites

R. Ortega-Zempoalteca[1], Y. Flores-Arias[1], G. Vázquez-Victorio[1], T. Gaudisson[2], S. Ammar[2], Z. Vargas-Osorio[1], U. Acevedo-Salas[1], and R. Valenzuela[*,1]

[1] Departmento de Materiales Metálicos y Cerámicos, Instituto de Investigaciones en Materiales, Universidad Nacional Autónoma de México, México D.F. 04510, México
[2] Laboratoire ITODYS, Université Paris-Diderot, Sorbonne Paris Cité, CNRS-UMR-7086, 75205 Paris cedex, France

Received 27 November 2013, revised 23 December 2013, accepted 9 January 2014
Published online 10 February 2014

Keywords ferrite nanoparticles, ferromagnetic resonance (FMR), spark plasma sintering (SPS)

[*] Corresponding author: e-mail raulvale@yahoo.com, Phone: +52 55 5622 4653, Fax: +52 55 5616 1371

Magnetic nanoparticles (NPs) of magnetite and Ni–Zn ferrites, synthesized by the forced hydrolysis in a polyol method, were used as the starting material to consolidate them by means of the spark plasma sintering (SPS) method. The microstructural changes were analyzed by X-ray diffraction, transmission electron microscopy (TEM), magnetic hysteresis loops, and ferromagnetic resonance (FMR) measurements. FMR spectra changed from a high resonance field and small linewidth for the nanoparticles to a spectrum with reduced resonance field with extremely broadened linewidths for the consolidated materials. These effects can be ascribed to the evolution from super-paramagnetic NPs to the formation of a nanostructured ceramic structure with high grain-to-grain interactions and with increased randomly distributed anisotropy axes.

1 Introduction Spinel nanoparticles (NPs) have recently attracted both scientific and technological interest by their structure, magnetic properties, and actual and potential applications. Magnetic properties in the nanometric scale have provided a wide variety of behaviors, mainly due to the fact that several magnetic critical dimensions (or lengths) fall within the nanometric range (1–100 nm). Several transitions involving a dramatic change in magnetic properties, such as the single to multidomain structure, the ordered to superparamagnetic behavior, take place in most ferrites at this size range [1]. Among the most interesting applications of magnetic NPs, we can mention the biomedical aimed at the elimination of cancer tumors [2, 3], in the environment for polutant removal from soils and water [4, 5], high-density data storage [6], and spintronics [7].

For many applications in electronic devices, a solid, high density material is needed, instead of a powder. However, the classic sintering techniques lead to a rapid grain growth, thereby losing the unusual magnetic properties associated with the nanometric scale. A promising novel technique to consolidate NPs powders into high density ceramics maintaining a grain size within the limits of the nanoscale is spark plasma sintering (SPS) [8]. SPS technique allows the fabrication of high-density samples at significantly lower temperatures and sintering times than the classic methods, often with improved magnetic properties [9, 10]. The SPS method can be used not only for consolidation of powders, but also for *in situ* solid state reactions [11].

In this paper, representative spinel ferrites NPs (magnetite and some Ni–Zn ferrites) are synthesized by the polyol method [12], and are subsequently consolidated by SPS under different sintering conditions. In addition to the microstructural methods [X-ray diffraction, transmission electron microscopy (TEM)], the effects of the SPS process are assessed by means of magnetic hysteresis loops and ferromagnetic resonance (FMR) measurements; the latter is an extremely sensitive tool. Dramatic changes are observed on the FMR parameters (resonance field, linewidth), which are interpreted in terms of variations in the internal magnetic field, and the randomly oriented anisotropic axes. These fundamental magnetic parameters change as a consequence of the formation of a polycrystalline structure in the consolidated materials.

2 Experimental techniques To synthesize spinel ferrites by the polyol method [12, 13], the corresponding metal acetates are dissolved in an alcohol (typically diethylenglycol) and brought to the boiling point under mechanical stirring. In order to obtain an oxide, a given amount of water is added to the reaction solution prior to heating. The reaction is maintained in reflux for a few hours. Once cooled down, the NPs are recuperated by centrifugation, washed in ethanol and dried at 80 °C in air.

In the SPS method [8], the starting material (usually a powder) is compressed in a graphite die; to increase the temperature, high intensity electric pulses are applied to the die. The reaction chamber is kept in a vacuum, or in a controlled atmosphere. The electric current flows through the die, and also through the sample if it is conductor. Recent results point to an enhancement of atom diffusion driven by the electric flux. But even in the case of insulating samples, the effects of the electrical field are believed to favor atomic diffusion [14]. The main result is that SPS can consolidate powders by sintering temperatures and times extremely low as compared with the classic solid state reactions. In this paper, a DR. Sintering 515 Syntex SPS facility (Thiais, France) was used.

A Siemens D-5000 diffractometer equipped with a cobalt source ($\lambda = 1.79030$ Å) was used to obtain the patterns. TEM was carried out using a JEOL-100-CX II microscope operating at 100 kV. Hysteresis loops were measured at room temperature in a LDJ 2600 VSM magnetometer with a maximum magnetic field of 16 kOe. FMR spectra were obtained in a Magnettech Miniscope MS 400, with an operation frequency of 9.4 GHz (X-band). In this system, the AC microwave field is perpendicular to the low-sweeping H field.

3 Experimental results and discussion We first examine the results obtained on magnetite. The NPs obtained by the polyol method showed an X-ray diffraction pattern (Fig. 1) of a spinel structure with a unit cell ($a = 8.396 \pm 0.002$ Å), very close to that of bulk magnetite ($a = 8.3940$ Å [15]), with broad diffraction peaks. These broadened diffraction peaks are associated with nanoparticles in the nanometric range. TEM micrographs (Fig. 2) exhibited a NP size about 8 nm. The magnetization of these NPs was measured in the ZFC–FC (zero-field-cooled and field-cooled) modes, leading to a superparamagnetic graph (Fig. 3) with a blocking temperature about 170 K, deduced from the maximum in the zero-field-cooled plot.

The superparamagnetic behavior can be explained on a simplified basis by considering that the total magnetocrystalline anisotropy energy, E_K, depends on the product of the nanoparticle volume times its magnetocrystalline constant, K, [16],

$$E_K = K\,V \tag{1}$$

where V is the NP volume. When the thermal energy, $k_B T$ (with k_B being Boltzmann constant) approaches E_K, thermal energy dominates over anisotropy and the magnetization becomes randomly oriented. In the case of spinel ferrites, where the magnetization is the resulting vector from the contribution of two sublattices (tetrahedral and octahedral), it is this resulting magnetization vector, which exhibits a

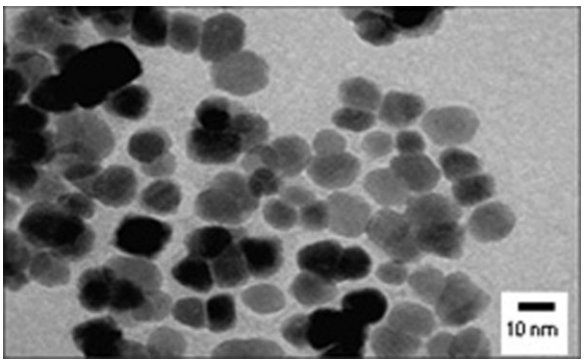

Figure 2 TEM micrograph of magnetite NPs.

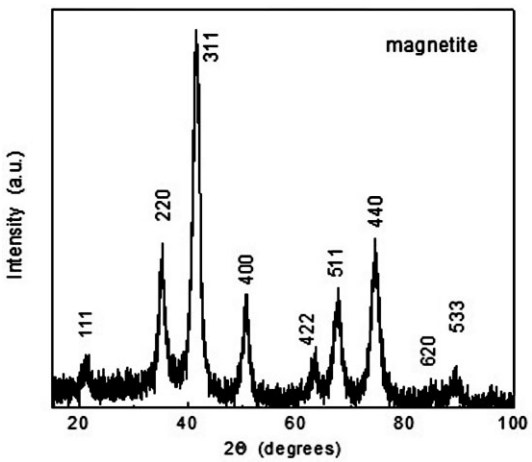

Figure 1 X-ray diffraction pattern of magnetite NPs obtained by the polyol method.

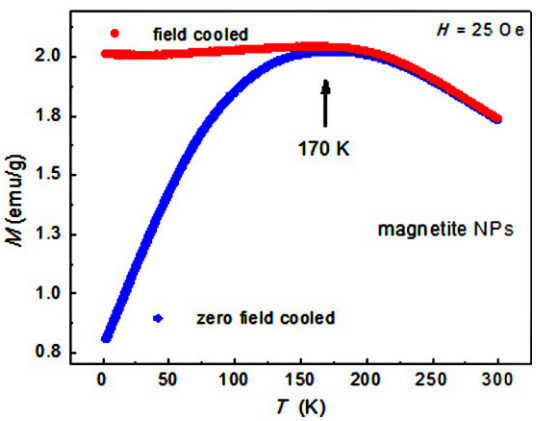

Figure 3 ZFC–FC magnetization measurements on the magnetite NPs obtained by the polyol method.

randomly oriented behavior in the superparamagnetic state. This magnetic state in ferrites (particularly in magnetite) has attracted a lot of interest for potential biomedical applications [17]. A superparamagnetic ensemble of nanoparticles possess no remanent magnetization and thus magnetic interactions between NPs disappear, preventing aggregation within blood vessels. When a magnetic field is applied, in contrast, a significant magnetization appears allowing transport of such NPs by means of the magnetic field.

These NPs were subsequently consolidated by SPS, at 750 °C for 15 min. A strong change in the FMR spectrum was observed (Fig. 4); the NPs spectrum showed a high resonance field and a small linewidth (3112 and 533 Oe, respectively), while the consolidated magnetite exhibited the effects of ferrimagnetic ordering, with a resonance field, H_{res}, of 1363 Oe and a broadened linewidth, ΔH, of 1456 Oe. In fact, the signal extends considerably in the high field section. The SPS-magnetite has larger grains (about 150 nm), with strong interactions, leading to a ferrimagnetic behavior.

As it was mentioned in the previous section, high current applied during the SPS method promotes an extremely efficient cation diffusion which allows a very fast sintering. In the case of magnetite, we have shown [18] that magnetite samples consolidated by SPS at 750 °C for 15 min have exhibited a clear Verwey transition resolved on its two components: the crystallographic transition from monoclinic to cubic, and the spin reorientation due to the change in anisotropy from uniaxial below 120 K, to cubic [111] for temperatures above 120 K [19].

The broadening of the linewidth can be associated with the presence of randomly distributed anisotropy axes from one grain to its neighbors. This distribution is especially wide in the case of most ferrites, due to the fact that they possess cubic [111] easy directions.

The change in FMR spectra of $Ni_{1-x}Zn_xFe_2O_4$ spinel ferrites with several compositions x, from the NPs state synthesized by the polyol method to the ceramic microstructure as produced by SPS was also studied. Figure 5 shows the temperature profile applied to $x = 0.7$ NPs to consolidate them at 600 °C for 10 min. The effects on the FMR spectrum appear in Fig. 6, exhibiting a strong decrease in resonance field, as well as an increase in the linewidth. In spite that both magnetite and $x = 0.7$ NPs are in the superparamagnetic state, the NPs spectrum appears with a linewidth even smaller for the latter, simply because the Curie temperature for this composition is quite lower (~340 K), than for magnetite (~858 K) [15]. When measuring both at room temperature, the $x = 0.7$ spinel is very close to the Curie transition, $T/T_C = 0.88$, while for magnetite, $T/T_C = 0.35$. The corresponding hysteresis loops are shown in Fig. 7. The as-produced NPs (blue) exhibit a typical superparamagnetic behavior with no coercive field (nor remanent magnetization), and a rounded progression toward saturation as the magnetic field increases.

We carried out a study on the effects of time and temperature of the SPS process, on the FMR spectra of $x = 0.5$ Ni–Zn ferrites. The consolidation of NPs by SPS is significant even at sintering temperatures as low as 350 °C and times as short as 10 min. Figure 8 shows the FMR spectra

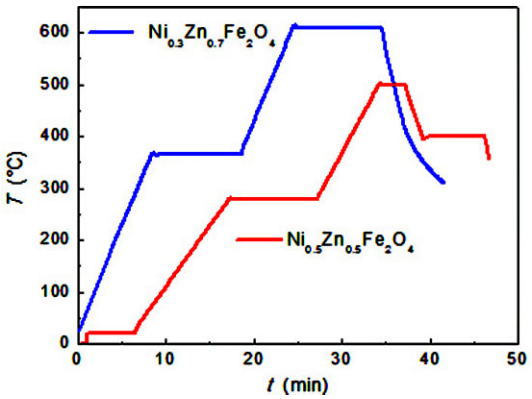

Figure 5 Temperature profile for the SPS process of $x = 0.7$ (blue) and 0.5 (red) Ni–Zn ferrites.

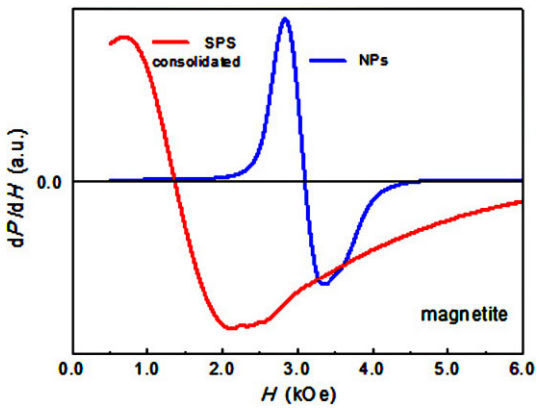

Figure 4 FMR spectra of magnetite NPs as-prepared (blue), and after the SPS process. Measurements at 300 K.

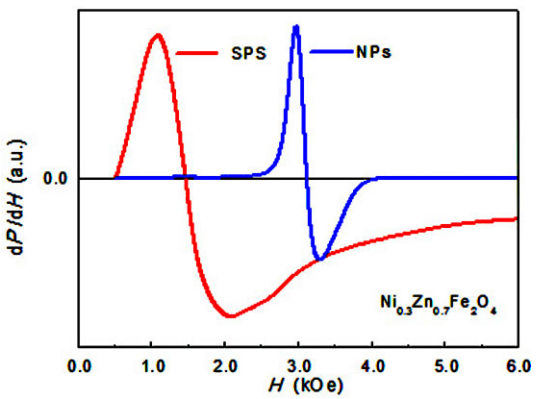

Figure 6 FMR spectra of NiZn NPs with $x = 0.7$ (blue), and SPS sintered at 600 °C 10 min (red), at 300 K.

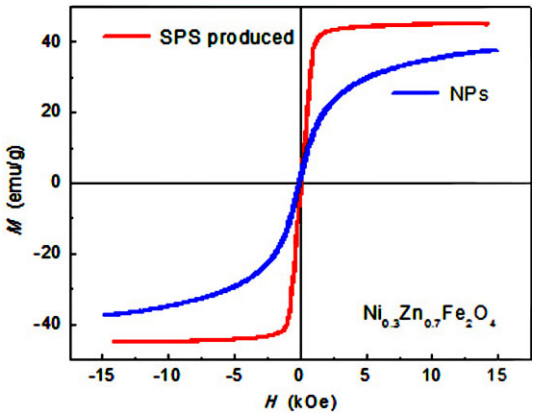

Figure 7 Magnetic hysteresis loops of $x = 0.7$ NPs Ni–Zn ferrites as produced by the polyol method (blue), and after consolidation by the SPS method (red). Measurements at 300 K.

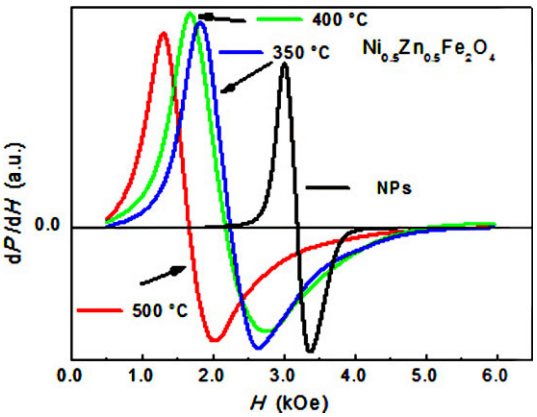

Figure 9 FMR spectra of $x = 0.5$ NiZn ferrites SPS sintered at different temperatures. The as-produced NPs spectrum (black) is also shown for comparison. Measurements at 300 K.

for 10 and 20 min of sintering time. The resonance field decreases and the linewidth increases. Also, the spectrum for $t_{sint} = 10$ min exhibits a slightly inhomogeneous resonance line probably associated with the progressing changes in the microstructure. As consolidation proceeds, some local differences in grain size, porosity, etc. can have an influence on the internal field.

Spinel NPs with the same composition ($x = 0.5$) were sintered by SPS at 400 and 500 °C; the temperature profile for the latter appears in Fig. 5. The temperature is raised up to 500 °C (after a de-gassing step at 280 °C to eliminate any organic remaining from the polyol reaction) for 5 min, and then lowered to 400 °C for an extra 5 min. This procedure allows an increase in density with very small grain growth. The final grain size in these materials is typically in the 80–120 nm.

We have gathered all the FMR spectra for this composition, including the NPs, in Fig. 9. The resonance field and the linewidth tendency observed in the previous compositions is found again: the superparamagnetic NPs appear with the largest H_{res} and the smaller ΔH (see Table 1), and a progressive decrease of the former and decrease of the latter is observed as the sintering temperature increases. The decrease in the resonance field is originated by an increase in the internal field, as a consequence of the grain growth, the formation of grain boundaries, and the increase in the grain-to-grain exchange interactions. This leads to ferrimagnetic behavior.

The shift in resonance field can be interpreted in terms of a significant increase in the internal magnetic field. In the Larmor equation [20],

$$\omega = \gamma H_{eff}, \tag{1}$$

where ω is the angular frequency, γ the gyromagnetic ratio, and H_{eff} the total magnetic field on the resonance spins. In the case of magnetically ordered materials, in addition to the applied field there is an internal field, H_{int},

$$H_{eff} = H_{int} + H_{ext}, \tag{2}$$

which includes all the contributions associated with magnetic ordering:

$$H_{int} = H_{exch} + H_{demag} + H_{anis} + H_{dip} \tag{3}$$

where H_{exch} is the field due to the exchange interactions, H_{demag} the demagnetization field, H_{anis} the field due to the

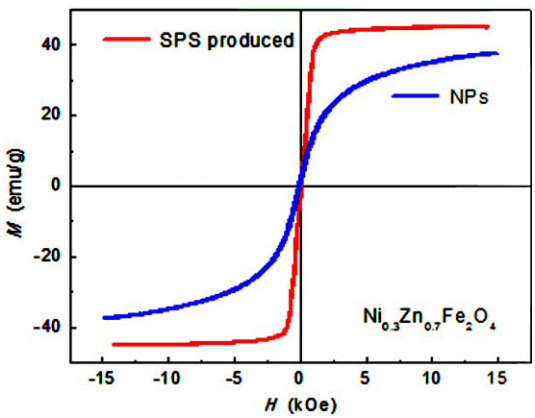

Figure 8 FMR measurements on $x = 0.5$ NPs ferrites after a SPS sintering at 350 °C for 10 (blue) and 20 min (red). Measurements at 300 K.

Table 1 FMR parameters of samples in Fig. 9.

sample	resonance field (Oe)	linewidth (Oe)
NPs	3210	370
SPS 350 °C	2262	818
SPS 400 °C	2180	1082
SPS 500 °C	1676	730

magnetocrystalline anisotropy, H_{dip} the field originated by dipolar interactions between NPs or grains.

The shift in the resonance field due to the increase in anisotropy between the NPs and the consolidated body can be estimated, in a very approximate way, by an expression derived from the Kittel formulae [21],

$$H_{res} = \frac{h\nu}{g\mu_B} - \frac{2K_1}{M_s}, \quad (4)$$

where H_{res} is the shifted resonance field, h is the Planck's constant, ν is the microwave frequency, g is the Landé factor, μ_B is the Bohr magneton, K_1 is the magnetocrystalline constant, and M_s is the saturation magnetization. This expression assumes a uniaxial anisotropy, which is not the case for these ferrites, but can give an estimation. A calculation of the increase in anisotropy between the as-produced NPs and the corresponding consolidated body by SPS was made for magnetite, and also for the case of $x = 0.7$ Ni–Zn ferrites (Figs. 4 and 6). The results, $K_1 \sim 42\,kJ\,m^{-3}$ for magnetite, and $K_1 \sim 18\,kJ\,m^{-3}$ for $x = 0.7$ NiZn clearly seem too high to represent solely the anisotropy contribution; for bulk magnetite, $K_1 = -11\,kJ\,m^{-3}$ [15] (the minus sign is due to the fact that anisotropy is cubic in magnetite). The conclusion is that the shift in resonance field has other contributions than just the increase in magnetocrystalline anisotropy.

The broadening of the linewidth for SPS-consolidated samples has been observed in other ferrites, such as Co–Zn [22] ferrites and Zn ferrites [23], and has been modelled by assuming that the main contribution for such broadening is the random distribution of anisotropy axes [24]. The spectra are numerically calculated with a macro-spin model for single domain NPs using Landau–Lifshitz–Gilbert dynamics. A qualitative agreement with experimental data has been observed.

4 Conclusions Magnetic NPs of spinel ferrites (magnetite and Ni–Zn of various compositions) were consolidated by SPS, at temperatures and sintering times extremely low as compared with the typical sintering conditions in the solid state technique. The SPS allows a significant increase in density with very limited grain growth. The obtained microstructures were studied by FMR at room temperature. The main results indicate a shift in the resonance field as compared with the starting NPs, and a broadening of the linewidth, especially at applied fields larger than the resonance field. Such broadening is originated by an increase in magnetocrystalline anisotropy between the superparamagnetic state and the ferromagnetic consolidated samples, and the associated random distribution of anisotropy axes in the high density samples. This random distribution is more important in spinel ferrites, as most of these materials have cubic anisotropy. Finally, FMR is a very sensitive tool for the investigation of nanostructured magnetic materials.

Acknowledgements Authors acknowledge support from ANR (France)-CONACyT) México grant # 139292 and DGAPA-UNAM PAPIIT grant IN101412. ZFC-FC experiments were carried out at the Iberian International Laboratory, Braga, Portugal. The collaboration of Prof J. Rivas and Dr. M. Bañobre-López is acknowledged.

References

[1] P. Guimaraes, Principles of Nanomagnetism (Springer-Verlag, Berlin, 2009), pp. 4–6.
[2] L. Harivardhan Reddy, J. L. Arias, J. Nicolas, and P. Couvreur, Chem. Rev. **112**, 5818 (2012).
[3] H. M. Joshi, J. Nanopart. Res. **15**, 1235 1–19 (2013).
[4] S. C. N. Tang and I. M. C. Lo, Water Res. **47**, 2613 (2013).
[5] Y.-M-. Hao, C. Man, and Z. B. Hu, J. Hazard. Mater. **184**, 392 (2010).
[6] D. Sellmyer and R. Skomski, Advanced Magnetic Nanostructures (Springer-Verlag, New York, 2006).
[7] S. D. Bader, Rev. Mod. Phys. **78**, 1 (2006).
[8] R. Orru, R. Lichen, A. M. Locci, and G. Cao, Mater. Sci. Eng. R **63**, 127 (2009).
[9] N. Millot, S. Le Gallet, D. Aymes, F. Bernard, and Y. Grin, J. Eur. Ceram. Soc. **27**, 921 (2007).
[10] S. Imine, F. Schenstein, S. Mercone, M. Zaghirioui, N. Bettahar, and N. Jouini, J. Eur. Ceram. Soc. **31**, 2943 (2011).
[11] L. Wang, J. Zhang, and W. Jiang, Int. J. Refract. Met. **39**, 103 (2013).
[12] S. Chkoundali, S. Ammar, N. Jouini, F. Fievet, M. Richard, P. Molinie, F. Villain, and J. M. Greneche, J. Phys. Condens. Matter **16**, 4357 (2004).
[13] H. Basti, L. Ben Tahar, L. S. Smiri, F. Herbst, M. J. Vaulay, F. Chau, S. Ammar, and S. Benderbous, J. Colloid Interface Sci. **341**(2Co), 248 (2010).
[14] Z. A. Munir, U. Anselmi-Tamburini, and M. Ohyanagi, J. Mater. Sci. **41**, 763 (2006).
[15] R. Valenzuela, Magnetic Ceramics (Cambridge University Press, Cambridge, 2005), p. 8.
[16] X. Battle, and A. Labarta, J. Phys. D Appl. Phys. **35**, R15 (2002).
[17] B. Issa, I. M. Obaidat, B. A. Albiss, and Y. Haik, Int. J. Mol. Sci. **14**, 21266 (2013).
[18] T. Gaudisson, G. Vázquez-Victorio, M. Bañobre-López, S. Nowak, J. Rivas, S. Ammar, F. Mazaleyrat, and R. Valenzuela, J. Appl. Phys. **115**, 17E117 (2014).
[19] V. Skumryev, H. J. Blythe, J. Cullen, and J. M. D. Coey, J. Magn. Magn. Mater. **196–197**, 515–517 (1999).
[20] C. Corvaja, in: Electron Paramagnetic Resonance: A practitioner's toolkit, edited by M. Brustolon and E. Giamello (Wiley, New York, 2009), chap. 1.
[21] C. Kittel, Phys. Rev. **73**, 155 (1948).
[22] R. Topkaya, A. Baykal, and A. Demir, J. Nanopart. Res. **15**, 1359 (2013).
[23] G. Thirupathi and R. Singh, IEEE Trans. Magn. **48**, 3630 (2012).
[24] A. Sukhov, K. D. Usadel, and U. Nowak, J. Magn. Magn. Mater. **320**, 31 (2008).

